# Hyperfine-structure measurements of the $^{151,153}Eu^+$ ground state

O. Becker, K. Enders, and G. Werth
*Institut für Physik der Universität Mainz, Staudingerweg 7, D-6500 Mainz, Germany*

J. Dembczynski
*Instytut Fizyki, Politechnika Poznanska, PL-60-965 Poznan, Poland*
(Received 4 May 1993)

The laser rf double-resonance technique in a Paul trap has been used to make high-precision measurements of the hyperfine structure (hfs) of the $4f^7(^8S_{7/2})6s\ ^9S_4$ ground state in $^{151,153}Eu^+$. We have obtained linewidths below 1 kHz for the magnetic-field-dependent rf transitions at frequencies between 1.7 and 10 GHz. After corrections for the second-order hfs we obtain values for the magnetic-dipole, electric-quadrupole, magnetic-octupole, and electric-hexadecapole interaction constants.

PACS number(s): 35.10.Fk, 32.30.Bv, 32.80.Pj

## I. INTRODUCTION

The hyperfine structure of different levels in atomic and ionic europium has been the subject of several investigations in recent years. The reason is that the two stable isotopes of mass 151 and 153 are a prominent example of a nuclear shape transition which manifests itself in a exceptionally large isotope shift and in a large difference in the nuclear magnetic-dipole and electric-quadrupole moments [1]. Much effort has been devoted to precise measurements of the hfs in different metastable levels of the singly charged ion using collinear laser and rf spectroscopy. Sen *et al.* [2] have measured the hfs in the $4f^7(^8S_{7/2})5d\ ^9D_4$ state and obtained uncertainties of 1 and 10 kHz in the $A$ and $B$ hfs constants, respectively. A similar precision was reported in a following experiment by Sen and Childs on the $4f^7(^8S_{7/2})5d\ ^9D_{2,3,5}$ states [3]. Villemoes *et al.* extended the measurements to the $4f^7(^8S_{7/2})5d\ ^9D_6$ and the $4f^7(^8S_{7/2})6p_{3/2}$; $J=5$ levels [4].

The $4f^7(^8S_{7/2})6s\ ^9S_4$ ground state has attracted much less consideration due to the experimental difficulty of optically existing resonance lines that are in the near uv spectral range. Guthöhrlein [5] has measured the ground-state hfs with optical interferometric precision, which was not sufficiently accurate to determine electric quadrupole coupling constants $B$.

We have performed an ion-trap experiment on the $Eu^+$ ground state. This technique has been demonstrated to be extremely powerful in cases where the ionic level structure is rather simple as in the alkali-metal-like ions [6]. Uncertainties below 1 Hz in the several GHz hfs splitting are often attained. Most recently the technique has been extended to $^{207}Pb^+$ with similar precision, although this ion offers only a very weak $M1$ transition for optical excitation [7]. The high precision is made possible by the fact that in all these cases the electronic angular momentum $J=1/2$ couples to a half-integer nuclear spin, resulting in an integer total angular momentum $F$. Therefore, a Zeeman sublevel $m_F=0$ exists, which is independent of residual stray magnetic-field fluctuations and inhomogeneities inside the trap to first order. In contrast, the nuclear spin of $I=5/2$ and the electronic angular momentum $J=4$ in $^{151,153}Eu^+$ couple to yield half-integer quantum numbers $F$. Consequently no $m_F=0$ level exists and all Zeeman sublevels depend on the residual magnetic field to first order. The precision then depends on the degree to which the residual magnetic field can be shielded or canceled. As it is shown below, however, little effort is necessary to obtain linewidths of a few kHz or below, which still enables the determination of hfs coupling constants with great precision.

## II. EXPERIMENT

### A. Trapping

The ions are confined in a Paul trap of 2 cm radius, driven by a rf oscillator at $\omega/2\pi=500$ kHz of 550 V amplitude. They are created by surface ionization from a platinum filament located near the inner surface of one trap electrode. Two holes in the ring electrode of 4 mm diameter serves as an entrance and an exit of a laser beam for ion excitation. The upper end-cap electrode is formed by a mesh (60% transmission) to allow the observation of fluorescence light from the ion cloud. The base pressure in our apparatus is about $10^{-9}$ mbar after bakeout at 350 °C. In order to achieve sufficiently long storage times we introduce buffer gas into our apparatus to damp the ion motion inside the trap and to compensate for energy gain from the time-varying electric trapping fields. Using $N_2$ at about $2\times10^{-4}$ mbar as a buffer gas, we obtain storage times of about 1 day. Typical ion numbers are $10^5$–$10^6$.

### B. Optical spectrum

A prerequisite for an optical-microwave double-resonance experiment is the resolution of the different hyperfine components in the optical spectrum to allow selective excitation of a given hyperfine sublevel. We ex-

 ©1993 The American Physical Society

cite the resonance transition from the $4f^7(^8S_{7/2})6s\ ^9S_4$ ground state to the $4F^7(^8S_{7/2})6p_{3/2}$, $J=5$ excited state at 382 nm for optical excitation. We used a tuneable narrow-band (0.5 MHz) ring dye laser operated with polyphenyl 2 as dye and pumped by an uv-argon-ion laser, which delivered up to 40 mW single-frequency output power. The excited state partially decays into the metastable $4f^7(^8S_{7/2})5d\ ^9D_6$ level, emitting 664.5-nm photons (Fig. 1). This fluorescence was used to monitor the ground-state population of the stored ions, allowing detection virtually free from stray laser light. The total count rate at resonance was 10 kHz with a total efficiency of our optical detection system of $10^{-4}$ which includes finite solid angle (5%), filter and transmission losses (10%), and quantum efficiency of the Ga-As photomultiplier. The dark current was reduced to a few Hz by cooling the photomultiplier tube.

Figure 2 shows the experimental setup and Fig. 3 an optical excitation spectrum of a natural mixture of $Eu^+$ isotopes. The linewidth is about 2 GHz, which is just sufficient to identify the individual hyperfine components. From the Doppler width we derive an ion temperature of 2200 K.

### C. Optical pumping

Tuning the laser to one of the hyperfine components in the optical spectrum, the corresponding ground-state hyperfine level will be depleted by optical pumping within a few ms. The laser excited state decays either into one of the different ground-state hyperfine levels or into one of the metastable $D$ states. In the latter case, the ion will be removed from the pumping cycle for a time corresponding to the lifetime of this state. While this lifetime has not been determined, from our experiment we conclude that it is as large as many seconds. This reduces the signal-to-noise ratio substantially. In order to return ions from the metastable states into the ground state we use collisions with background gas molecules for quenching. We found that $N_2$ as a buffer gas at a pressure of about $2\times10^{-4}$ mbar reduces the effective $D$-state lifetime sufficiently. On the other hand, it does not lead to a substantial relaxation between the ground-state hyperfine levels, which would reduce the population difference created by optical pumping.

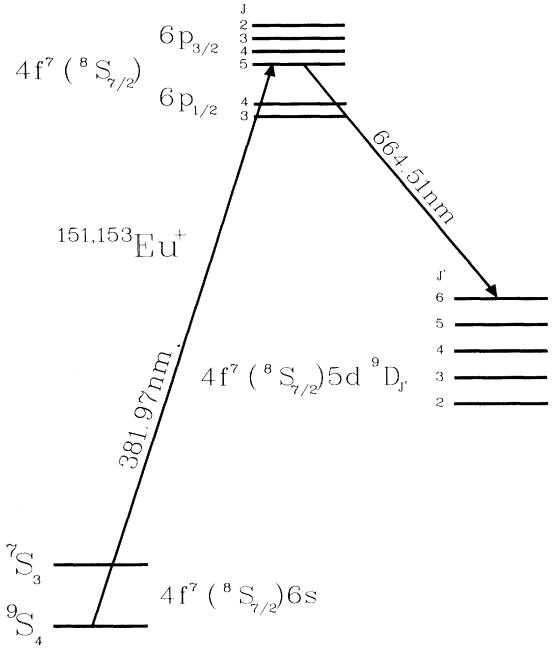


FIG. 1. Partial energy-level diagram of $Eu^+$.

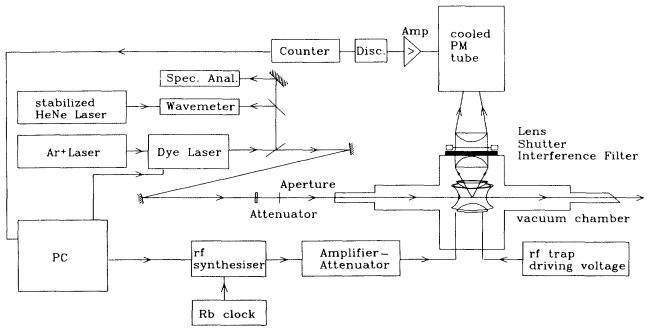


FIG. 2. Diagram of experimental apparatus for laser-microwave double-resonance experiment on $Eu^+$ in a Paul ion trap.

### D. Microwave transitions

Microwaves are transmitted into the apparatus using the ion-source filament as antenna. This gives sufficient power at the position of the ion inside the trap. They are produced by a frequency synthesizer, whose time base is controlled by a Rb atomic clock.

When we sweep the microwave frequency across a hyperfine resonance we observe an increase in fluores-

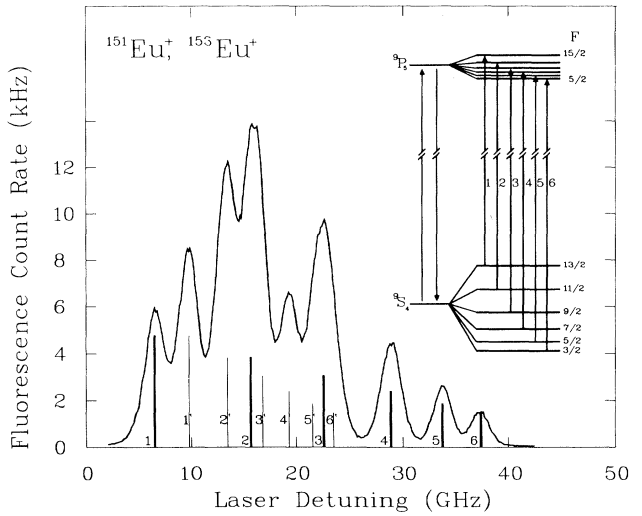


FIG. 3. Optical $^9S_4$-$^9P_5$ excitation spectrum of a natural mixture of $Eu^+$ ions. The positions of the different hyperfine components are indicated by thick ($^{151}Eu^+$) and thin ($^{153}Eu^+$) bars. The Doppler linewidth corresponds to an ion temperature of 2200 K.

cence intensity, since the population of the optically pumped hyperfine level increases by population transfer from the resonantly coupled neighboring level. From the $\Delta F=\pm 1$ selection rule there are five different hyperfine transition frequencies between the levels $F=13/2$ and $F=3/2$ for each isotope. Every transition is split into Zeeman sublevels by the residual magnetic stray field at the ion position. Using three mutually perpendicular Helmholtz coils, which are limited in size to 10 cm radius by the experimental setup, we achieved a average magnetic field of 270 mG over the ion cloud volume of about 1 $cm^3$. Because this field is inhomogeneous, in some cases we are not able to completely resolve the $\Delta m_F=\pm 1$ components of the transitions because of their large dependence on the magnetic field. However, the central component, corresponding to the $\Delta m_F=0$ selection rule, is well resolved in all cases. Figure 4 shows as an example the $F=13/2$ to $F'=11/2$ transition in $^{151}Eu^+$ at 10 GHz. Figure 5 shows the innermost two components of the $\Delta m_F=0$ manifold of the transition in Fig. 4 at higher resolution.

As a second example, Fig. 6 shows the $F=5/2$ to $F'=3/2$ transition in $^{151}Eu^+$ at 3.8 GHz. Here the $\Delta m_F=0, \pm 1$ components overlap because of the $g_F$ factors for this set of quantum numbers and all possible lines are well resolved. The quantity of interest is the center of the Zeeman pattern giving the desired hyperfine transition frequency. For a precise determination of this frequency we usually restricted our measurements to the innermost lines symmetrically around the center as in Fig. 5. In most cases the linewidth of these components could be reduced below 1 kHz and the experimental points could be well fitted by a Lorentzian. We believe that the limiting factor in linewidth is the residual $B$-field inhomogeneity. The linewidth $\delta\nu$ would then be $\delta\nu=(g_F-g_{F'})\mu_B\delta B$. In fact, we observe for a given B field a linear increase of $\delta\nu$ with increasing distance of the individual Zeeman transition from the center. The statistical uncertainty of the center frequency from the fit typically is (5–10)% of the linewidth. As an example, the statistical uncertainty of the $F=13/2$ to $F'=11/2$ hyperfine frequency from the lines of Fig. 5 is 22 Hz.

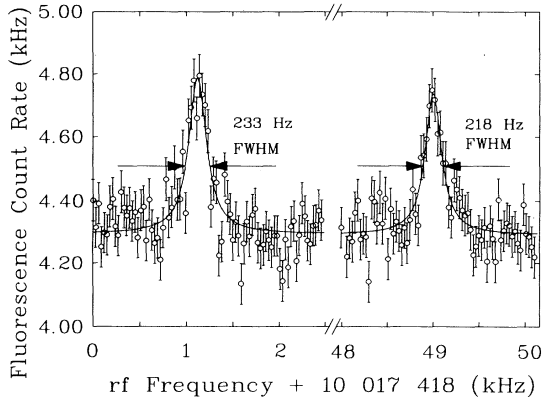


FIG. 5. The two innermost lines of Fig. 4 with high resolution. The statistical uncertainty of the central hfs frequency, determined from these lines, is 22 Hz.

## III. EXPERIMENTAL RESULTS

From the center of the observed Zeeman pattern, we derived the hyperfine transition frequencies for all possible $\Delta F=1$ transitions for both isotopes. These frequencies must be corrected for a small quadratic Zeeman effect, which can be calculated with sufficient accuracy from second-order perturbation theory using the $g_F$ value obtained from pure $LS$ coupling. Most of these corrections are of the order of a few Hz and are in general smaller than the statistical uncertainties. Table I gives our experimental results including these corrections.

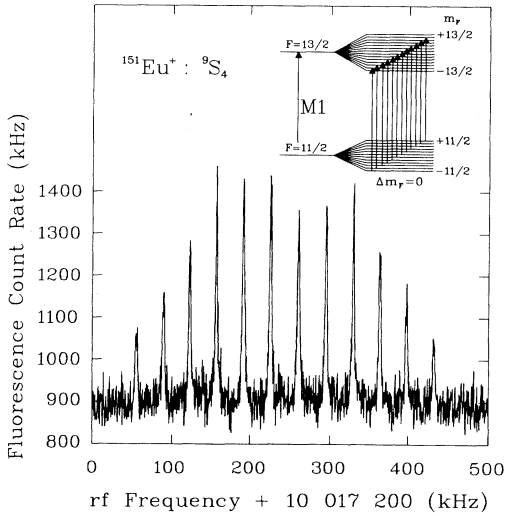


FIG. 4. $\Delta m_F=0$ component of the Zeeman transitions between the $F=13/2$ and $F=11/2$ ground-state hyperfine level in $^{151}Eu^+$. The residual magnetic field at the ion position was 270 mG.

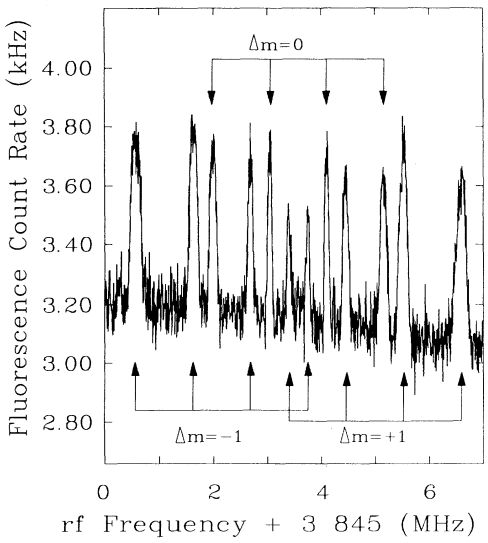


FIG. 6. $\Delta m_F=0,\pm 1$ Zeeman transitions between the $F=5/2$ and $F=3/2$ ground-state hyperfine levels in $^{151}Eu^+$. Because of the large $g$ factor the $\Delta m_F=\pm 1,0$ components overlap.

TABLE I. Measured transition frequencies in $4f^7(^8S)6s\ ^9S_4$ ground-state hyperfine structure of $Eu^+$ corrected by the second-order Zeeman shift (column 3). Column 5 gives the final second-order hfs corrections corresponding to the fit number VI in Table II. The last column gives the differences between experimental frequencies and the calculated ones using the fitted parameters of VI in Table II.

| Isotope | Transition $F$-$F'$ | Frequency (Hz) | Expt. freq. error (Hz) | Second-order hfs corr. (Hz) | (Expt)−(Fit) (Hz) |
|---|---|---|---|---|---|
| $^{151}Eu^+$ | 13/2-11/2 | 10 017 442 828 | 22 | −5 831 871 | 0 |
| | 11/2-9/2 | 8 473 144 121 | 105 | −1 547 373 | 26 |
| | 9/2-7/2 | 6 930 424 679 | 57 | 1 040 890 | −20 |
| | 7/2-5/2 | 5 388 995 721 | 183 | 2 243 683 | 249 |
| | 5/2-3/2 | 4 848 568 018 | 150 | 2 370 352 | −84 |
| $^{153}Eu^+$ | 13/2-11/2 | 4 449 976 109 | 70 | −1 151 697 | 0 |
| | 11/2-9/2 | 3 765 315 459 | 101 | −305 715 | 5 |
| | 9/2-7/2 | 3 080 679 446 | 111 | 205 486 | −17 |
| | 7/2-5/2 | 2 396 063 741 | 187 | 443 128 | 59 |
| | 5/2-3/2 | 1 711 463 310 | 210 | 468 221 | −37 |

TABLE II. The hfs coupling constants for the magnetic-dipole ($A$), electric-quadrupole ($B$), magnetic-octupole ($C$), and electric-hexadecapole ($D$) interaction in the ground state $4f^7(^8S)6s;^9S_4$ of the two stable isotopes $^{151}Eu^+$ and $^{153}Eu^+$. The fit numbers correspond to I, uncorrected hfs constants; II, corrected for the magnetic-dipole hfs interaction with the $^7S_3$ state only; III, corrected for $M1$ and $E2$ hfs interactions with the state $^7S_3$ only; IV, additional changes of differences $E(^7S_3)-E(^9S_4)$ by taking the $F$ dependence into account; V, added hfs interactions with other $J=3$ states; VI, added hfs interactions with the state $^7D_5$ and $^7F_5$, final results.

| Fit No. | hfs constant | $^{151}Eu^+$ (Hz) | $^{153}Eu^+$ (Hz) | $^{151}Eu^+$:$^{153}$ $Eu^+$ |
|---|---|---|---|---|
| I | $A$ | 1 540 476 486(12) | 684 601 369(5) | 2.250 180 26(2) |
| | $B$ | 8 910 554(231) | 137 400(86) | 64.85(4) |
| | $C$ | 466(22) | 66(8) | 7.1(9) |
| | $D$ | −6(5) | −5(2) | 1.2(1.1) |
| II | $A$ | 1 540 297 161(12) | 684 565 948(5) | 2.250 034 73(2) |
| | $B$ | −653 445(231) | −1 751 726(86) | 0.373 03(13) |
| | $C$ | 466(23) | 66(8) | 7.1(9) |
| | $D$ | −6(5) | −5(2) | 1.2(1.1) |
| III | $A$ | 1 540 297 163(12) | 684 565 951(50 | 2.250 034 73(2) |
| | $B$ | −653 519(230) | −1 751 808(86) | 0.373 05(13) |
| | $C$ | 455(23) | 54(7) | 8.4(1.2) |
| | $D$ | −6(5) | −5(2) | 1.2(1.0) |
| IV | $A$ | 1 540 297 283(12) | 684 565 962(9) | 2.250 034 87(3) |
| | $B$ | −656 137(231) | −1 752 030(85) | 0.374 50(13) |
| | $C$ | 24(23) | 17(7) | 1.4(1.5) |
| | $D$ | −6(5) | −5(2) | 1.2(1.1) |
| V | $A$ | 1 540 297 264(12) | 684 565 959(5) | 2.250 034 85(2) |
| | $B$ | −656 878(231) | −1 752 215(84) | 0.374 88(13) |
| | $C$ | 36(23) | 14(7) | 2.6(2.1) |
| | $D$ | −6(5) | −5(2) | 1.2(1.1) |
| VI | $A$ | 1 540 297 394(13) | 684 565 993(9) | 2.250 034 927(35) |
| | $B$ | −660 862(231) | −1 752 868(84) | 0.377 02(13) |
| | $C$ | 26(23) | 3(7) | 9(22) |
| | $D$ | −6(5) | −5(2) | 1.2(1.1) |

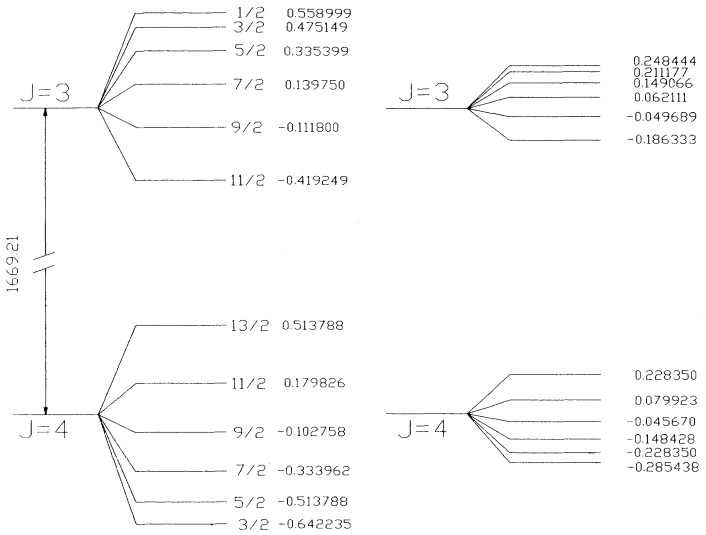


FIG. 7. Hyperfine structure of the $^9S_4$ and $^7S_3$ levels in $^{151}Eu^+$ and $^{153}Eu^+$. All energies are given in $cm^{-1}$.

## IV. DETERMINATION OF THE hfs *A*, *B*, *C*, AND *D* CONSTANTS

Initially, the hyperfine parameters $A$ (magnetic dipole), $B$ (electric quadrupole), $C$ (magnetic octupole), and $D$ (electric hexadecapole) were linear-least-squares fitted to the data in Table I. The functional relationship between these parameters, level shifts, and the quantum numbers $I$, $J$, and $F$ are given by the formulas of Kopfermann [8] and Schwartz [9]. However, it is well known that the hfs interactions mix electronic states with different $J$ quantum numbers. This effect is especially strong for the ion $^{151}Eu^+$ and manifests itself in deviations from the Landè interval rule and, as shown below, an anomalously large $B$ constant.

Earlier measurements [3,10–12] have shown that the isotropic electric quadrupole hfs ratio $B(^{151}Eu)/B(^{153}Eu)$ is about 0.393. The ratio $Q(^{151}Eu)/Q(^{153}Eu)$ of the nuclear ground-state electric-quadrupole moments is conventionally assumed to be the same, since the quadrupole moments cannot be directly measured like the dipole moments. As can be seen from Table II, the first-order theory gives a ratio $B(^{151}Eu)/B(^{153}Eu)\approx 65$ that is completely inconsistent with the anticipated ratio of 0.393. The discrepancy cannot arise from imperfect knowledge of eigenvector compositions, which would alter the $B$ value for each isotope by the same factor and therefore leave the ratio unchanged. It must instead arise from second-order hyperfine effects, which can perturb hfs splittings by hyperfine interactions between the $|4f^7(^8S_{7/2})6s\ ^9S_4;F\rangle$ states and other atomic states. This effect is called "breakdown in $J$ as a good quantum number." In such a case secular equations should be constructed for an atomic structure, where only one quantum number $F$ representing a total angular momentum of the atom, is a good quantum number. The concept of atomic secular equations was first proposed by Casimir [13] and recently was successfully applied by Kronfeld *et al.* [14] for explanation of the hfs splittings in the neutral Eu term $e\ ^6D$ of $4f^7(^8S_{7/2})6s6d$. However, this procedure cannot be used for the analysis of our measurement because the differences between the hfs-sublevel energies of the $Eu^+$ ground state $^9S_4$ and the hfs-sublevel energies of the main perturbing state $4f^7(^8S_{7/2})6s\ ^7S_3$ have been measured only with optical interferometric precision [5], and therefore do not have sufficient precision for the analysis. Therefore, we used second-order perturbation theory to calculate the "repulsion effect" between different hfs sublevels with the same quantum number $F$. The second-order energy shift is given by

$$\delta W_F(\psi,J)=\frac{|\langle\psi,JIFm|H_{\rm hfs}|\psi',J'IFm\rangle|^2}{E(\psi,JF)-E(\psi',J'F)}\ , \tag{1}$$

where $|\psi\rangle=|\phi SL\rangle$ denotes the real fine-structure $SLJ$ state (wave function in intermediate coupling) written in $SL$ basis and $I,F,m$ are good quantum numbers characterizing the real hfs state.

The Hamiltonian operator $H_{\rm hfs}$ can be written as

$$H_{\rm hfs}=\sum_K T_N^K \sum_{\kappa,k}(T_{\rm el}^{(\kappa k)K}+X^{(\kappa k)K})\ , \tag{2}$$

where $T_N^K$ is the nuclear multipole-moment operator of order $K$ [15], $T_{\rm el}^{(\kappa k)K}$ is the electronic one-body hfs operator [15], and $X^{(\kappa k)K}$ is the two-body hfs operator (for more details see [16]).

In most cases [17], the denominator in Eq. (1) is limited to

$$E(\Psi,J)-E(\Psi',J')\ . \tag{3}$$

This approximation is not suitable in the case studied. As seen in Fig. 7, the sequence of hyperfine sublevels of the $^9S_4$ and the $^7S_3$ configuration are inverted. This requires, particularly for $^{151}Eu^+$ with larger hyperfine sublevel separations, taking into account the $F$ dependence of the energy differences.

The matrix element in the numerator of Eq. (1) can be expressed as a function of one- and two-body hfs radial parameters $a^k,b^k$ [10] and $a_i,b_i$ [16], respectively, when the calculations of the second-order effects are limited to

magnetic-dipole and electric-quadrupole hfs interactions. The values of these hfs radial parameters can be determined by semiempirical methods [16] using experimentally determined $A$ and $B$ constants.

The observed hfs splittings of the $^9S_4$ level is dominated by contributions from the $6s$ electron. The contributions of the $4f$ electrons to the hfs splittings are much smaller, however, they cannot be neglected in the interpretation of very-high-precision experimental data. To determine all contributions to $A$-, $B$-, $C$-, and $D$-hfs constants it is necessary to measure hfs splittings for several levels belonging to the same configuration. Unfortunately, for the $4f^76s$ configuration of $Eu^+$ sufficient information is not available. Only one excited level, $^7S_3$, of this configuration is known [18] with its $A$-hfs constant measured by Guthöhrlein [5]. Therefore, for the determination of hfs radial parameters, which are needed for calculations of the second-order corrections, we used measurements of hfs splittings of the level $^8S_{7/2}$ in neutral Eu performed by Sandars and Woodgate [10] and the results of Baker and Williams for the $^8S_{7/2}$ level in $Eu^{2+}$ [19].

The energy levels have been estimated using ratios of Hartree-Fock values for the Slater integrals, $F^k$, the values of the spin-orbit parameters $\zeta$, and the experimental energy values for the terms $4f^7\,^6P$ and $^6I$ of $Eu^{2+}$ and $4f^76s\,^7S$ of $Eu^+$. The radial spin-orbit parameter of neutral Eu as well as of $Eu^{2+}$ have been set to provide agreement between experimental and calculated $g$ factors of the $^8S_{7/2}$ levels. The resulting components of the intermediate wave functions needed for hfs interpretation are as follows.

(i) For the $Eu^{2+}$ ion

$$|4f^7\,^8S_{7/2}\rangle = 0.982\,415|4F^7\,^8S_{7/2}\rangle + 0.184\,771|4f^7\,^6P_{7/2}\rangle - 0.015\,107|4f^7\,^6D_{7/2}\rangle + 0.001\,332|4f^7\,^6F_{7/2}\rangle + \cdots . \quad (4)$$

(ii) For the neutral Eu

$$|4f^76s^2\,^8S_{7/2}\rangle = 0.984\,831|4f^76s^2\,^8S_{7/2}\rangle + 0.171\,922|4f^76s^2\,^6P_{7/2}\rangle - 0.013\,405|4f^76s^2\,^6D_{7/2}\rangle + 0.001\,114|4f^76s^2\,^6F_{7/2}\rangle + \cdots . \quad (5)$$

(iii) For the $Eu^+$ ion

$$|4f^7(^8S)6s;^9S_4\rangle = 0.982\,641|4f^7(^8S)6s;^9S_4\rangle + 0.183\,122|4f^7(^6P)6s;^7P_4\rangle - 0.003\,995|4f^7(^6D)6s;^5D_4\rangle - 0.014\,654|4f^7(^6D)6s;^7D_4\rangle + 0.000\,576|4f^7(^6F)6s;^5F_4\rangle + 0.001\,258|4f^7(^6F)6s;^7F_4\rangle + \cdots , \quad (6)$$

$$|4f^7(^8S)6s;^7S_3\rangle = 0.982\,013|4f^7(^8S)6s;^7S_3\rangle + 0.181\,359|4f^7(^6P)6s;^5P_3\rangle - 0.042\,496|4f^7(^6P)6s;^7P_3\rangle - 0.014\,466|4f^7(^6D)6s;^5D_3\rangle + 0.006\,310|4f^7(^6D)6s;^7D_3\rangle + 0.001\,216|4f^7(^6F)6s;^5F_3\rangle - 0.000\,826|4f^7(^6F)6s;^7F_3\rangle + \cdots . \quad (7)$$

Using these eigenvector amplitudes to form the matrix elements of the hfs operator (2), one obtains theoretical expressions for the hfs constants. Since the participation of the $4f$ electrons in the hfs of the levels $^9S_4$ and $^7S_3$ is small, the two-body hfs effects involving these electrons have been neglected (effect of excitations from open shells into empty shells [20]). In our case, only the two-body hfs effects involving the $6s$ electron (excitations from closed $n''s$ shells into open $6s$ shells and open $6s$ shells into empty $n's$ shells) are important. These effects have been parametrized in the same way as has been done for the $3d^n4s$ configuration [16]. Hence, the hfs constants of interest are expressed as follows:

$$A(Eu^+;^9S_4) = 0.008\,467\,56a_{4f}^{01} + 0.002\,542\,66a_{4f}^{12} + 0.866\,532\,74a_{4f}^{10} + 0.125\,000\,03a_{6s}^{10} + 0.001\,209\,65a_{9,10} , \quad (8)$$

$$A(Eu^+;^7S_3) = 0.011\,230\,22a_{4f}^{01} + 0.003\,390\,42a_{4f}^{12} + 1.113\,767\,50a_{4f}^{10} - 0.124\,998\,78a_{6s}^{10} - 0.284\,091\,0a_{9,10} , \quad (9)$$

$$A(Eu;^8S_{7/2}) = 0.008\,671\,66a_{4f}^{01} + 0.002\,566\,68a_{4f}^{12} + 0.991\,223\,08a_{4f}^{10} , \quad (10)$$

$$A(Eu^{2+};^8S_{7/2}) = 0.010\,051\,02a_{4f}^{01} + 0.002\,842\,07a_{4f}^{12} + 0.989\,809\,12a_{4f}^{10} - 0.282\,802\,51a_{9,10} , \quad (11)$$

$$B(Eu^+;^9S_4) = 0.001\,733\,46b_{4f}^{02} + 0.000\,062\,78b_{4f}^{13} + 0.055\,058\,03b_{4f}^{11} , \quad (12)$$

where $a_{4f}^{01}$, $a_{4f}^{12}$, $a_{4f}^{10}$, $a_{6s}^{10}$ $b_{4f}^{02}$, $b_{4f}^{13}$, and $b_{4f}^{11}$ are the familiar radial parameters (one-body parameters) [15], $a_{9,10}$ is the two-body hfs parameter defined as follows [16]:

$$a_{9,10} = \frac{16\pi\mu_B g_I}{3h}\left\{\sum_{n'\geq 7}^{\infty}\langle f|C^3|s\rangle^2 R^3(4f6s,n's4f)\psi_{6s}(0)\psi_{n's}(0) - \sum_{n''=1}^{5}\langle f|C^3|s\rangle^2 R^3(4f6s,n''s4f)\psi_{6s}(0)\psi_{n''s}(0)\right\}\Big/\Delta E . \quad (13)$$

TABLE III. The hfs radial parameters used for calculations of second-order corrections.

| Radial parameter | $^{151}Eu^+$ (MHz) | $^{153}Eu^+$ (MHz) |
|---|---|---|
| $a_{4f}^{01}$ | 916(20) | 404(9) |
| $a_{4f}^{12}$ | 982 | 433 |
| $a_{4f}^{10}$ | −30.79(80) | −13.60(30) |
| $a_{6s}^{10}$ | 12450.88(80) | 5533.25(31) |
| $a_{9,10}$ | 298.56(3) | 132.66(2) |
| $b_{4f}^{02}$ | 833.4(3.5) | 2210.6(3.5) |
| $b_{4f}^{13}$ | 83.3 | 221.0 |
| $b_{4f}^{11}$ | −38.4 | −101.7 |

The radial parameter $a_{4f}^{10}$ used above is defined for the configuration $4f^7 6s^2$ in neutral Eu. The differences in definition of the core-polarization effects for the $Eu^+$ and for the $Eu^{2+}$ have been taken into account by use of the two-body hfs parameters $a_{9,10}$.

We take experimental values of the $A$ and $B$ constants for $^9S_4$ ($Eu^+$) obtained in this work and results from other authors including the states $^7S_3$ ($Eu^+$) [5], $^8S_{7/2}$ (Eu) [10], and for the $^8S_{7/2}$ in $Eu^{2+}$ [19] into account. Using these values in Eqs. (8)–(12) results in the one- and two-body hfs radial parameters given in Table III. Moreover, according to the relativistic self-consistent-field calculations of Lindgren and Rosen 15] the following relations

TABLE IV. Values of second-order corrections for the hfs sublevels of the state $^9S_4$ of the isotope $^{151}Eu^+$ (a) and $^{153}Eu^+$ (b). *, theoretically predicted level energy value in $cm^{-1}$; I, correction for magnetic-dipole hfs interaction with the $^7S_3$ state only; II, correction for $M1$ and $E2$ hfs interaction with the $^7S_3$ state only; III, additional changes of differences $E(^7S_3)-E(^9S_4)$ taking the $F$ dependence into account.

(a)

Second-order corrections for hfs sublevels in $^{151}Eu^+$ (Hz)

| Perturbing state | | $F=13/2$ | $F=11/2$ | $F=9/2$ | $F=7/2$ | $F=5/2$ | $F=3/2$ |
|---|---|---|---|---|---|---|---|
| $^7S_3$ | I | 0 | 5 828 062 | 7 377 943 | 6 340 420 | 4 098 857 | 1 729 205 |
| | II | 0 | 5 828 121 | 7 377 949 | 6 340 377 | 4 098 806 | 1 729 176 |
| $^7S_3$ | III | 0 | 5 830 214 | 7 377 989 | 6 338 578 | 4 096 721 | 1 728 020 |
| $^7P_3$ | $E=27\,336$* | 0 | 328 | 410 | 349 | 224 | 94 |
| $^5P_3$ | $E=28\,077$* | 0 | 5 | 6 | 5 | 3 | 1 |
| $^7D_3$ | $E=34\,817$* | 0 | 178 | 212 | 172 | 106 | 43 |
| $^5D_3$ | $E=35\,848$* | 0 | 10 | 12 | 10 | 6 | 3 |
| $^7F_3$ | $E=49\,600$* | 0 | 1 | 2 | 1 | 1 | 0 |
| $J=3$ | total | 0 | 5 830 736 | 7 378 631 | 6 339 115 | 4 097 061 | 1 728 161 |
| $^7D_5$ | $E=34\,377$* | 3823 | 4952 | 4433 | 3065 | 1444 | 0 |
| $^7F_5$ | $E=49\,000$* | 19 | 25 | 23 | 16 | 8 | 0 |
| | total | 3842 | 5 835 713 | 7 383 086 | 6 342 196 | 4 098 513 | 1 728 161 |

(b)

Second-order corrections for hfs sublevels in $^{153}Eu^+$ (Hz)

| Perturbing state | | $F=13/2$ | $F=11/2$ | $F=9/2$ | $F=7/2$ | $F=5/2$ | $F=3/2$ |
|---|---|---|---|---|---|---|---|
| $^7S_3$ | I | 0 | 1 151 186 | 1 457 326 | 1 252 390 | 809 626 | 341 561 |
| | II | 0 | 1 151 253 | 1 457 333 | 1 252 341 | 809 567 | 341 528 |
| $^7S_3$ | III | 0 | 1 151 437 | 1 457 337 | 1 252 183 | 809 384 | 341 426 |
| $^7P_3$ | $E=27\,336$* | 0 | 69 | 81 | 66 | 41 | 17 |
| $^5P_3$ | $E=28\,077$* | 0 | 1 | 1 | 1 | 1 | 0 |
| $^7D_3$ | $E=34\,817$* | 0 | 48 | 43 | 26 | 13 | 4 |
| $^5D_3$ | $E=35\,848$* | 0 | 2 | 2 | 2 | 1 | 0 |
| $^7F_3$ | $E=49\,600$* | 0 | 0 | 0 | 0 | 0 | 0 |
| $J=3$ | total | 0 | 1 151 557 | 1 457 464 | 1 252 278 | 809 440 | 341 447 |
| $^7D_5$ | $E=34\,377$* | 866 | 1005 | 813 | 515 | 226 | 0 |
| $^7F_5$ | $E=49\,000$* | 4 | 5 | 5 | 3 | 2 | 0 |
| | total | 870 | 1 152 567 | 1 458 282 | 1 252 796 | 809 668 | 341 447 |

between radial hfs parameters have been assumed:

$$\frac{a_{4f}^{12}}{a_{4f}^{01}}=1.071\ ,\quad \frac{b_{4f}^{13}}{b_{4f}^{02}}=0.100\ ,\quad \frac{b_{4f}^{11}}{b_{4f}^{02}}=-0.46\ . \quad (14)$$

Using the intermediate-coupling wave functions for the perturbed state $|4f^7(^8S)6s;^9S_4\rangle$ and also for the perturbing states $|4f^7v_1s_1L_16s;^{2S+1}L_J\rangle$ with $J=3$ and 5, and the values of the hfs radial parameters given in Table III, the second-order corrections, Eq. (1), have been calculated and are given in Tables IV(a) and IV(b).

The nonlinear correction (1) cannot be implemented in the linear fit routine used for the solution of the linear expansion of the hfs interaction. Therefore an iterative procedure was applied, starting with a preliminary set of hfs one- and two-body radial parameters. The hfs radial parameters are used to explicitly calculate the resulting energy shifts $W_F$ of every hfs sublevel under study. These shifts are used to correct the measured rf transitions, which leads to corrected $A$, $B$, $C$, and $D$ constants. The corrected $A$ and $B$ constants are then used for the determination of the hfs radial parameters of the next iterative step. This procedure converges to a final set of hfs radial parameters and the final corrected $A$, $B$, $C$, and $D$ constants, listed in Table II.

## V. DISCUSSION

We have determined the ground-state hyperfine splitting of both stable isotopes of $Eu^+$ with great precision. The experiment demonstrates that spectroscopy in ion traps, which so far has been restricted to ions with simple alkali-metal-like level schemes, can successfully be extended to complex level structures. From our magnetic-dipole interaction constants we derive a precise value of the hyperfine anomaly

$$^{151}\Delta^{153}=\left[\frac{A(^{151}Eu^+)}{A(^{153}Eu^+)}\right]\left[\frac{\mu(^{153}Eu^+)}{\mu(^{151}Eu^+)}\right]-1$$
$$=-0.006\,63(18)$$

when we use the ratio of the nuclear magnetic moments $\mu_I$ from [21]. We note, that $Eu^+$ is a good candidate for a systematic investigation of differential hyperfine anomaly, since it has seven unstable isotopes with lifetimes exceeding several days, which could be investigated off line from the production area. The high accuracy of this measurement technique is more than sufficient for detailed, precise studies of the hyperfine anomaly.

We have determined the ratio $B(^{151}Eu^+)/B(^{153}Eu^+)$ of the quadrupole interaction constants to be 0.377 02(13). This agrees well with measurements of the ratio of quadrupole moments in muonic atoms $Q(^{151}Eu^+)/Q(^{153}Eu^+)=0.3744(53)$ [22], it disagrees, however, from other spectroscopic determinations of the $B$ factors in different atomic states of Eu and $Eu^+$ as recently compiled by Möller *et al.* [12]. It can be seen from Table IV that the main contribution to the second-order corrections originates from the magnetic-dipole hfs interaction with the state $|4f^7(^8S)6s;\ ^7S_3\rangle$. Inclusion of the electric-quadrupole hfs interaction (denoted by II in Table IV) changes the second-order corrections insignificantly. Similarly, if we take into account $M1$ and $E2$ hfs interactions with other $J=3$ and $J=5$ states (Table IV), the changes are also insignificant. Moreover, introducing these interactions does not change the ratio $B(^{151}Eu^+)/B(^{153}Eu^+)$ within the quoted errors, as seen in Table II.

The coupling constants for the magnetic-octupole interaction obtained by our analysis are small and can be taken as zero within our limits of error. An anomalously large "pseudo-octupole" coupling constant could be induced by the approximation $\Delta E=E(\psi,J,F)-E(\psi',J',F)\approx E(\psi,J)-E(\psi',J')$ in cases where the nuclear magnetic moment $\mu_I$ is large and $\Delta E$ is small ($\approx$1000–2000 $cm^{-1}$). If, e.g., we take the differences $E(^7S_3,F)-E(^9S_4,F)$ into account, the calculated $C$ constants are reduced from 466 to 24 Hz for $^{151}Eu^+$ and from 66 to 17 Hz for $^{153}Eu^+$ as seen in Table II.

In our analysis of the hyperfine splitting we find a value for the electric-hexadecapole interaction constant $D$, which is significantly different from zero. To our knowledge, this is the second time that such a value has been determined; the first observation was by Dankwort and Penselin [23]. The hexadecapole hfs constant $D$ is not significantly affected by the $M1$ and $E2$ hfs interactions between electronic states with different $J$ quantum numbers. These $D$ constants can be affected only if the $M3$ interaction is strong. We have simulated the influence of the hfs octupole interaction on the values of the second-order corrections. Using $\Omega=1$ nmb for the nuclear octupole moment, we obtained changes of the calculated corrections below 1 Hz. Hence, the values obtained for the $D$ constants, in particular for $^{153}Eu^+$, can be considered as the "true" hfs hexadecapole constants. This is also confirmed by the fact that the obtained values for $D$ constants are independent from the included second-order corrections (see Table II).

The accuracy of the second-order corrections could be improved by high-precision hfs measurements for the $^7S_3$ level and if the energy separation $E(^7S_3)-E(^9S_4)$ was better known. The hfs data for the $^7S_3$ state would influence the obtained values of the hfs radial parameters, and as consequence, calculated second-order corrections. The impact on the values of the coupling parameters, however, would be small.

## ACKNOWLEDGMENTS

Part of this work was supported by the Deutsche Forschungsgemeinschaft and by the KBN, Poland, under Project No. 2P302 05204. We thank F. Arbes for help on the early stages of the experiment, E. Stachowska for checking of calculations, and B. Bushaw for critically reading the manuscript.

[1] S. A. Ahmad *et al.*, Z. Phys. A **321**, 35 (1985).
[2] A. Sen, L. S. Goodman, W. J. Childs, and C. Kurtz, Phys. Rev. A **35**, 3145 (1987).
[3] A. Sen and W. J. Childs, Phys. Rev. A **36**, 1983 (1987).
[4] P. Villemoes, A. Arnesen, F. Heijkenskjöld, A. Kastberg, and A. Wännström, Phys. Lett. A **162**, 178 (1992).
[5] G. Guthöhrlein, Z. Phys. **214**, 332 (1968).
[6] G. Werth, Comments At. Mol. Phys. **28**, 229 (1993).
[7] X. Feng, G. Z. Li, and G. Werth, Phys. Rev. A **46**, 2959 (1992).
[8] H. Kopferman, *Nuclear Moments* (Academic, New York, 1958).
[9] C. Schwartz, Phys. Rev. **97**, 380 (1955).
[10] P. G. H. Sandars and G. P. Woodgate, Proc. R. Soc. London Ser. A **275**, 269 (1960).
[11] W. J. Childs, Phys. Rev. A **44**, 1523 (1991).
[12] W. Möller, H. Hühnermann, G. Alkhazov, and V. Panteleev, Phys. Rev. Lett. **70**, 541 (1993).
[13] H. Casimir, *On the Interaction between Atomic Nuclei and Electrons* (Teylors Tweede Genootshap XI, Haarlem, 1936).
[14] H. D. Kronfeld, D. J. Weber, J. Dembczynski, and E. Stachowska, Phys. Rev. A **44**, 5737 (1991).
[15] I. Lindgreen and A. Rosen, Case Stud. At. Phys. **4**, 93 (1974).
[16] J. Dembczynski, W. Ertmer, U. Johann, and P. Unkel, Z. Phys. A **321**, 1 (1985).
[17] B. K. Woodgate, Proc. R. Soc. London Ser. A **293**, 117 (1966).
[18] W. C. Martin, R. Zalubas, and L. Hagan, *Atomic Energy Levels,* Natl. Bur. Stand. (U.S.) Circl. No. 60 (U.S. GPO, Washington, DC, 1978).
[19] J. M. Baker and F. I. B. Williams, Proc. R. Soc. London Ser. A **267**, 283 (1962).
[20] L. Armstrong, Jr., *Theory of the Hyperfine Structure of Free Atoms* (Wiley-Interscience, New York, 1971).
[21] L. Evans, P. G. H. Sandars, and G. K. Woodgate, Proc. R. Soc. London Ser. A **289**, 114 (1965).
[22] Y. Tanaka *et al.*, Phys. Rev. Lett. **51**, 1633 (1983).
[23] W. Dankwart and S. Penselin, Z. Phys. **267**, 229 (1974).